Multispecies expression of coccolithophore vital effects with changing CO_2 concentrations and pH in the laboratory with insights for reconstructing CO_2 levels in geological history

Goulwen Le Guevel[1][2], Fabrice Minoletti[1], Carla Geisen[2], Gwendoline Duong[3], Virginia Rojas[1] and Michaël Hermoso[2]

[1]Institut des Sciences de la Terre de Paris (UMR 7193 ISTeP), CNRS, Sorbonne Université, 75005 Paris, France
[2]Laboratoire d'Océanologie et de Géosciences (UMR 8187 LOG), Université du Littoral Côte d'Opale, CNRS, Université de Lille, 62930 Wimereux, France
[3]Laboratoire d'Océanologie et de Géosciences (UMR 8187 LOG), Université de Lille, CNRS, Université du Littoral Côte d'Opale, 62930 Wimereux, France

Correspondence to: Michael Hermoso (michael.hermoso@univ-littoral.fr)

Abstract. The coccolith sedimentary and micropalaeontological archive has fostered great interest for palaeoclimate applications. Indeed, the geochemistry of coccolith calcite has the potential to reconstruct both palaeo-CO_2 concentrations and palaeo-temperature of seawater. Studying coccolith geochemistry aims at better understanding the changes in the vital effect of coccoliths with changes in environmental parameters, especially the carbonate chemistry of seawater. To this aim, we need to deconvolve the biological imprint from the environmental signals recorded in the composition of coccolith biominerals. We have undertaken large-scale culture experiments of four strains of coccolithophores of various sizes and growth rates, grown under eight CO_2/pH conditions typifying the long-term CO_2 evolution of the Cenozoic Era. We propose an assessment of the expression of the vital effects for *Emiliania huxleyi*, *Gephyrocapsa oceanica*, *Helicosphaera carteri* and *Coccolithus braarudii* with simultaneous changes in Dissolved Inorganic Carbon (DIC) and pH in the medium resulting in variations in $CO_{2\,aq}$ availability to the cells. We have identified a distinct isotopic response of *C. braarudii* to pCO_2 levels on either side of the 600 ppmv (pH 7.89) condition. We propose that this discrepancy is the result of a modification of the proton efflux across the plasma membrane (voltage-dependent proton channels). We further show that as the CO_2 level rises and pH decreases (from 200 to 500 ppmv and from 8.29 to 7.96 pH units, respectively), a significant increase in $\delta^{13}C_{coccolith}$ of *C. braarudii* is expressed, along with a coeval decrease in $\delta^{13}C_{org}$. The constant physiological parameters of *C. braarudii* (growth rate, PIC, POC) across the 200 to 500 ppmv interval support the idea that the change in $\delta^{13}C_{coccolith}$ is only a consequence of a lower fractionation between dissolved CO_2 and organic matter. Meanwhile, the small (less carbon-limited) cells of *E. huxleyi* and *G. oceanica* do not exhibit any change in their carbon vital effects with changes in carbonate chemistry of the environment across the whole CO_2 spectrum. Using this new biogeochemical framework, we have established a calibration between $CO_{2\,aq}$ concentration and the differential vital effect ($\Delta\delta^{13}C$) between isotopically-invariant small *G. oceanica* and large coccoliths *C. braarudii*, whose vital effect is CO_2-dependent at low CO_2. The CO_2-$\Delta\delta^{13}C$

transfer equation allows palaeo-pCO$_2$ reconstructions based on isotope changes explained by physiological processes, especially at low and medium CO$_2$ levels.

1 Introduction

The atmospheric concentration of carbon dioxide (pCO$_2$) is a key parameter controlling global climate through its radiative forcing on Earth's surface temperatures. The reconstruction of past pCO$_2$ is challenging to handle as many caveats exist in the palaeo-CO$_2$ barometry methods. The magnitude of the carbon isotope fractionation between membrane lipids called alkenones produced by the coccolithophores – found in sediments – and ambient aqueous CO$_2$ constitutes the basis of the foremost palaeo-pCO$_2$ proxy, referred to as $\varepsilon_{p\text{-alk}}$ (Pagani et al., 2010; Zhang et al., 2019, 2020). This approach has led to significant advances in the understanding of the past CO$_2$ concentration, but its application still has some limitations. Conversely to the coccolith archive, alkenone molecules are not ubiquitously preserved in marine sediments and the assessment of pCO$_2$ involves a cascade of calculations requiring assumptions made on the δ^{13}C value of CO$_{2\ aq}$. Furthermore, this method has recently been shown to overestimate pCO$_2$ below 270 ppmv (Badger et al., 2019), potentially leading to underestimated pCO$_2$ above 270 ppmv. Alongside this proxy, the boron isotope fractionation in foraminifera tests has increasingly been used to reconstruct palaeo-pH (Rae et al., 2021). Combined with another parameter of the carbonate chemistry system as DIC or alkalinity, and with temperature, palaeo-pH can be used for palaeo-pCO$_2$ reconstructions (Foster, 2008; Sanyal et al., 1995). This proxy also suffers from uncertainties due to the evaluation of δ^{11}B of past seawater among others unknown factors (Klochko et al., 2006; Tripati et al., 2011).

In this study, we investigated the fractionation of carbon and oxygen isotopes in phytoplanktonic organic matter and coccolith calcite driven by changes in the carbonate chemistry of coccolithophores culture media. We have conducted *in vivo* culture experiments, that provide a means to constrain the cellular and isotopic responses of coccolithophores to environmental changes. Our culture experiments were conducted to quantify the isotopic departure of coccoliths from inorganic calcite (vital effect). The latter only depends on physico-chemical parameters of the environment such as δ^{18}O$_{sw}$, δ^{13}C$_{CO2}$, temperature, salinity, and pH (Zeebe and Wolf-Gladrow, 2001). However, when calcite is biomineralised intracellularly, biological parameters such as growth rate, cell size, and the PIC/POC ratio - which refers to the distribution of carbon between particulate organic carbon (POC) and particulate inorganic carbon (PIC) produced by calcifying organisms - also influence this fractionation (Dudley et al., 1986; McClelland et al., 2017; Rickaby et al., 2010). The causes behind the changes in the isotopic fractionation between the different cellular compartments are to be investigated at various stages of carbon fixation. Aqueous CO$_2$, the main form of DIC entering coccolithophorid cells, diffuses through the plasma membrane via passive diffusion (Gutknecht et al., 1977). CO$_2$ diffusion is governed primarily by Fick's first law, but also by the specific conditions of the cell boundary layer on the external side of the plasma membrane (Reinfelder, 2011; Wolf-Gladrow and Riebesell, 1997). In addition to passive CO$_2$ diffusion, certain taxa of coccolithophores such as *Emiliania* possess CCMs (Carbon Concentration Mechanisms), allowing the intake of HCO$_3^-$ through active transmembrane transport

65 (Bach et al., 2013; Parker and Boron, 2013; Romero et al., 2004). As HCO_3^- is enriched in ^{13}C compared to CO_2, the greater acquisition of HCO_3^-, the higher $\delta^{13}C$ values in the intracellular DIC pool and ultimately the higher $\delta^{13}C$ of coccolith calcite. Once inside the cell, carbon is utilised by two main pathways: the fixation into organic matter via photosynthesis in chloroplasts and precipitation of calcite forming coccoliths within the coccolith vesicle. Carbon fixation into organic matter by the enzyme RuBisCO (ribulose 1,5-bisphosphate carboxylase/oxygenase) (Ellis, 1979) leads to fractionation as it

70 preferentially fixes the lighter isotopes (^{12}C) (Laws et al., 2001; Popp et al., 1998). Consequently, organic matter is relatively depleted in ^{13}C (very negative $\delta^{13}C_{org}$) compared to the carbon source and compared to the intracellular DIC pool (Bidigare et al., 1997; Guy et al., 1993; Rau et al., 1996). The fractionation induced by RuBisCO is one component of a more general fractionation between the $CO_{2\,aq}$ from the external environment and the organic matter synthesised within the cell, which leads to an enrichment, noted ε_p (Jasper and Hayes, 1990; Pagani et al., 1999). In addition to being dependent on the

75 fractionation associated with RuBisCO, ε_p is influenced by physiological parameters such as growth rate, cell size, and the presence of CCMs (Laws et al., 1995; Popp et al., 1998).

In this work, we provide both $\delta^{13}C_{coccolith}$ and $\delta^{13}C_{org}$ values with changes in pCO$_2$ and pH to explain the mechanisms responsible for the carbon isotope fractionation within the cell. The present study stems from several lines of evidence that the isotopic offset between coccoliths of different sizes conveys a specific pCO$_2$ signal as shown in sedimentary records by

80 the work of Bolton and Stoll (2013). This empirical observation has been repeatedly reported in culture data (Hermoso, 2015; Hermoso et al., 2016b; McClelland et al., 2017; Rickaby et al., 2010). This approach used to derive palaeo-CO$_2$ concentrations still needs to be fully constrained, although a proof of concept exists (Bolton and Stoll, 2013; Godbillot et al., 2022; Hermoso et al., 2016b, 2020; Tremblin et al., 2016). Modelling studies fed by culture data have identified and quantified the main forcing parameters behind the magnitude of carbon isotope vital effect in coccolith calcite: growth rate,

85 cell size, the partitioning of CO$_2$ in particulate inorganic matter and particulate organic matter (PIC/POC ratio), among other ancillary parameters (McClelland et al., 2017).

Four strains of geological-relevant coccolithophores, representing a wide diversity of growth rate and coccolith and cell sizes, were cultured to study how the composition of the culture medium (DIC, pH) influences the magnitude of coccoliths vital effects and to establish transfer functions between these vital effects and the aqueous CO$_2$ concentrations and pH. In

90 contrast with previous culture studies and to accurately mimicking the carbonate chemistry of the ocean through the Cenozoic Era, we cultured these calcifying microalgae with coupled pCO$_2$ and pH perturbations of the medium. The culture conditions varied from 200 ppmv/8.29 pH units (pre-industrial) to 1400 ppmv/7.55 pH units (thought to represent the Mid-Eocene levels) keeping all other parameters constant. Particular attention has been paid to conditions similar to those of the last 12 Myrs (narrow step of 100 ppmv for pCO$_2$ between 200 and 500 ppmv) because of the scarcity of available data.

2 Materials and methods

2.1 Strains

We cultured four coccolithophore strains kindly provided by the biological station of Roscoff: RCC1200 *Coccolithus braarudii*, RCC1323 *Helicosphaera carteri*, RCC1314 *Gephyrocapsa oceanica*, and RCC1256 *Emiliania huxleyi* (Figure 1). These species represent a wide range of coccolith taxa with various coccosphere and cell sizes. The rationale of this choice is that they belong to the most abundant groups found in Neogene pelagic sediments (Bolton et al., 2012; Claxton et al., 2022). If comparable with our own study (mode of culture, temperature, pH etc…), the results of previously-published biogeochemical work on the same species will be presented along with our own data in the figures.

RCC1200 *Coccolithus braarudii*   RCC1323 *Helicosphaera carteri*   RCC1314 *Gephyrocapsa oceanica*   RCC1256 *Emiliania huxleyi*
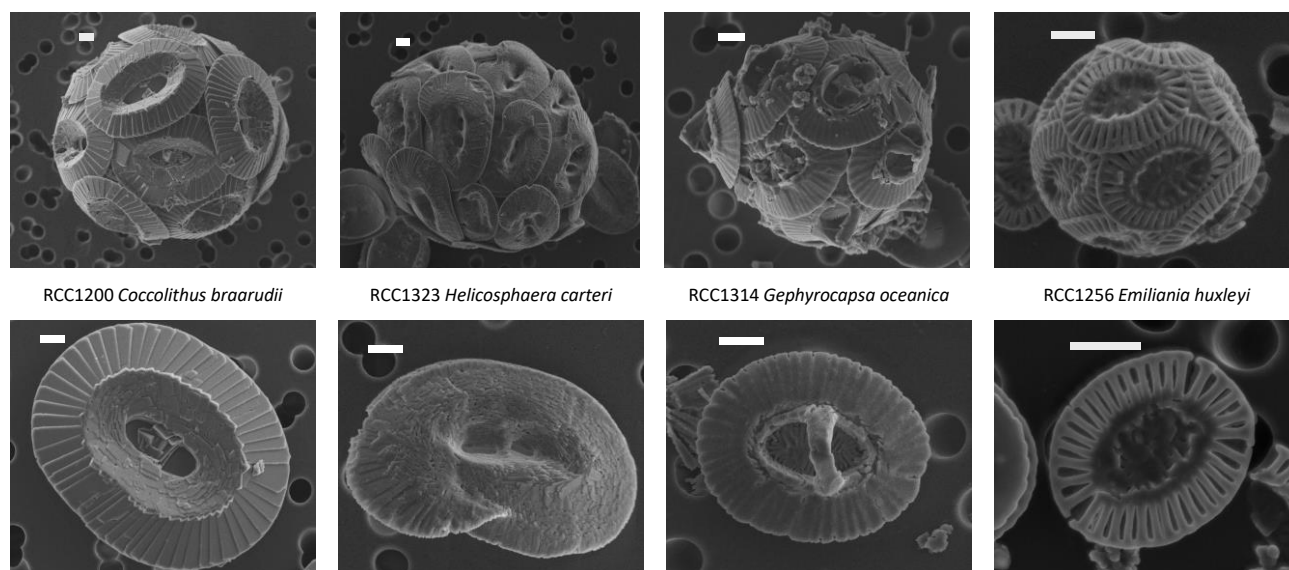
Figure 1: Scanning electron microscope (SEM) images of the four studied strains. Top images show the coccoliths and bottom images show the coccospheres. The scale bars represent 1 μm.

The cultures were undertaken at the Maison de la Recherche en Environment Naturel (ULCO - LOG) in Wimereux (Northern France) in 2023 – 2024.

2.2 Medium preparation

Our culture experiments were designed to represent pH and $p\text{CO}_2$ from the last greenhouse period (Eocene) to the preindustrial Holocene oceanic conditions (Rae et al., 2021; Sosdian et al., 2018). Variable $p\text{CO}_2$ between 200 and 1400 ppmv at constant alkalinity of 2300 μmol/kg have been used to calculate the target pH (total scale) with CO2sys program (Bakker et al., 2016) See table 1 for details on the chemical parameters of the culture medium.

4

115 Artificial seawater with a salinity of 34 psu was prepared following the ESAW recipe of Berges, Franklin and Harrison, (2001). The use of artificial seawater was preferred over natural seawater in order to facilitate the production of medium with CO_2 level under 400 ppmv. Phosphate, nitrate, silica, Fe-EDTA, trace metals and vitamins were added to produce K/2 media according to Keller et al. (1987). The DIC concentration was reached adding different amounts of $NaHCO_3$ (Sigma – batch CAS 144-55-8). The pH was adjusted with HCl and NaOH addition until the target pH was reached. This treatment led to a

120 change in the relative abundance of the DIC species (see Bjerrum plot of carbonate speciation versus pH, Zeebe and Wolf-Gladrow, 2001). Lastly, the medium was sterilised with a 0.22 μm filtration step and stored without headspace in amber-coloured bottles at 15 °C in the dark.

2.3 Culture growth

The coccolithophore strains were first acclimatised to the medium during about 10 generations in 25 cm^2 polystyrene flasks.

125 The cells were then inoculated in triplicate experiments in culture bottles of increasing size (75 cm^2 polystyrene flasks, 600 mL and 2300 mL polycarbonate bottles) until the target cell number of the culture was reached. We grew the cultures until reaching a sufficient biomass for our analyses (between 2 and 10 mg for the small cells *E. huxleyi* and *G. oceanica* and between 50 and 60 mg for the large cells *H. carteri* and *C. braarudii*), while ensuring that the cultures remained adequately diluted.

130 The cell cultures were maintained at constant temperature (15 °C) with a 14/10 day-length cyclicity and an irradiance of 150 μmol.photons.m^{-2}.s^{-1}. The cells were regularly resuspended to avoid cell clustering and kept at relatively low concentrations to maintain homogeneous carbon bioavailability and light access during all the experiment. A daily control of the culture health was made with a reverse optical microscope under x400 magnification. A final control of the coccoliths was made after the harvest with a Zeiss Supra 55 VP SEM at Sorbonne University.

135 Cell numeration and coccosphere sizes were measured using a Beckman Coulter Counter Multisizer 4e calibrated with 10.16 μm latex beads. The measurements were always performed at the same time of the day (8:30 to 10:00 am) to avoid biases related to the growth of the cell during the day phase.

The growth rate μ in day^{-1} of a microorganism culture corresponds to the increase of the cell number by time units commonly calculated with the formula:

140
$$\mu \ (day^{-1}) = \frac{ln(c_{final}) - \ln(c_{initial})}{t_{final} - t_{initial}}, \tag{1}$$

where c is the cell concentration and t_{final}-$t_{initial}$ is the number of days between the initial and the final cell concentration measurements. To take into account all the concentration measurements, the μ was derived from the slope of the linear regression of the function $f(t_x$-$t_{initial}) = ln(c_x)$ where x is the day of the measurement of c_x.

2.4 Isotopic reference of the culture medium

145 The $\delta^{13}C$ of the Dissolved Inorganic Carbon ($\delta^{13}C_{DIC}$) and the DIC concentrations were measured in 11 samples of various CO_2/pH with an Isotope and Gas Concentration Analyzer Picarro G2131-i coupled with an Apollo SciTech DIC-$\delta^{13}C$ analyser AS-D1 at LOCEAN laboratory (Sorbonne University). The medium samples were preserved in 500 mL glass bottle with ground neck with 0,3 mL saturated $HgCl_2$ solution. The measurements are calibrated with in-house standards. Since we used the same $NaHCO_3$ powder batch for the different experiments, all the culture media had the same $\delta^{13}C_{DIC}$ values (-

150 12.17‰ V-PDB (±0.07)).

The $\delta^{18}O$ of seawater was measured by cavity ring down spectroscopy (CRDS) using a Picarro instrument (model L2130-i Isotopic H_2O) at LOCEAN, Sorbonne University. The in-house standards (freshwater) are calibrated using IAEA references V-SMOW (Vienna Standard Mean Ocean Water) and GISP (Greenland Ice Sheet Precipitation). The $\delta^{18}O$ of the inorganic reference ($\delta^{18}O_i$) in ‰ V-PDB is calculated from the $\delta^{18}O_{sw}$ and temperature (15 °C) according to the equation of Kim and

155 O'Neil 1997 modified by Tremblin, et al. (2016). The $\delta^{18}O_{sw}$ slightly changed between successive culture campaigns: -6.44‰ V-SMOW (±0.03) for *C. braarudii* and *G. oceanica*, -6.67‰ V-SMOW (±0.03) for *H. carteri* and -6.36‰ V-SMOW (±0.15) for *E. huxleyi*).

The oxygen vital effects are calculated as the difference between the $\delta^{18}O$ of the coccoliths ($VE^{18}O$) in ‰ V-PDB and the $\delta^{18}O$ of a theoretical inorganic calcite ($\delta^{18}O_i$) in ‰ V-PDB:

160 $$VE^{18}O = \delta^{18}O_{coccoliths} - \delta^{18}O_i \, , \tag{2}$$

2.5 Isotopic analysis on calcite

Two methods were used to collect the culture residues for further isotopic measurements of coccolith calcite:

- RCC1200 *C. braarudii* and RCC1323 *H. carteri* culture residues were centrifuged during 15 minutes at 4500 rpm in 500 mL centrifuge bottles. After removing the supernatant, samples were rinsed with three cycles of centrifugation with

165 replacement of the supernatant with neutralised demineralised water and homogenisation between each cycle. The rinsing is employed to remove the salt from the culture water. The culture residues were finally dried at 40 °C after the removal of the last supernatant.

- RCC1256 *E. huxleyi* and RCC1314 *G. oceanica* samples were collected and rinsed three times with neutralised demineralised water onto polycarbonate filtering membranes, and then dried in a desiccator. We applied a different

170 harvesting method for those strains because of their small size, that induced too much material loss during the centrifugation process. All culture residues were stored at 5 °C after harvest.

Isotopic measurements on calcite were performed at the ISTeP laboratory (Sorbonne University). Between 30 and 60 µg of the samples were digested with 100% phosphoric acid at 70°C in pre-evacuated vials using a Kiel IV carbonate device. The evolved CO_2 was purified in a cryogenic trapping system and carbon and oxygen isotope compositions were measured in an

175 isotope-ratio mass spectrometer DELTA V advantage (Thermo Scientific) with a dual inlet introduction system. The carbon

and oxygen isotope composition were expressed in the delta notation as a value relative to the Vienna Pee Dee Belemnite (V-PDB) and reported in permil (‰). $\delta^{13}C$ and $\delta^{18}O$ values were calibrated using NBS-19 and NBS-18 international standards. Internal reproducibility and accuracy were monitored by replicate analysis of in-house calcite standard Marceau ($\delta^{13}C = 2.12‰$ and $\delta^{18}O = -1.87‰$), being the measured values for $\delta^{13}C$ and $\delta^{18}O$ 2.10 ±0.08‰ (1σ) and -1.89 ±0.10‰ (1σ),

180 respectively. The external reproducibility, obtained from replicate analysis of the samples, is better than 0.05‰ (1σ) for $\delta^{13}C_{coccolith}$ and 0.10‰ (1σ) for $\delta^{18}O_{coccolith}$. Transfer equations between coccolith isotope ratios and CO_2 levels are proposed in this study. The residual errors are evaluated through Monte Carlo analysis code with 1,000,000 iterations and an uncertainty of 0.17‰ for the differential vital effect between small and large coccolithes $\Delta\delta^{13}C_{small-large}$ (1σ).

2.6 Carbon isotope analysis of the organic matter

185 The culture residues of *C. braarudii*, *G. oceanica* and *E. huxleyi* were gathered onto glass microfiber filters (GFF), rinsed three times with neutralised demineralised water and then stored at -18 °C. We then gently scratched the superficial part of the GFF to collect all the culture residue. The culture residues were decarbonated with hydrochloric acid 2N overnight. The samples were then rinsed to eliminate the excess of hydrochloric acid and released Ca^{2+} and alkalinity, and then dried at 35 °C. Between 10 and 50 µg of decarbonated culture residues (only organic matter) were weighted and loaded into tin

190 capsules.

The carbon isotope composition of the organic matter was measured at the Stable Isotope Geochemistry laboratory at IPGP (Institut de Physique du Globe de Paris). A Flash EA 1112 elemental analyser coupled in continuous helium flow to an isotope ratio mass spectrometer Thermo Fisher Scientific DELTA V Plus was used for the *C. braarudii* samples cultured between 200 and 500 ppmv (8.29 and 7.96 pH units). For *G. oceanica* and *E. huxleyi* for all culture conditions, and for *C.*

195 *braarudii* between 500 and 1400 ppmv (7.96 and 7.55), we used an Elementar vario PYRO cube analyser coupled with the same spectrometer DELTA V Plus at IPGP. Three organic-rich internal standards, calibrated against international standards, were used to calculate the $\delta^{13}C$ values of the samples, reported in ‰ with respect to V-PDB. Replicate analysis of standards yielded an internal reproducibility better than 0.10‰ (1σ). Accuracy was assessed by measuring an in-house Tyrosine standard ($\delta^{13}C = -23.23‰$), for which the estimated error was better than 0.20‰. The external reproducibility for $\delta^{13}C_{org}$,

200 obtained from replicate analysis of the samples, is better than 0.07%.

2.7 Carbon content analysis

The PIC:POC ratios of the four strains studied under various pCO$_2$/pH conditions were measured at the Wimereux marine station using a Thermo Fisher Flash 2000 elemental analyzer. The culture residues were collected and stored in the same way for analyses of the $\delta^{13}C_{org}$. The calibration used for reconstructing carbon content was done with various amounts of

205 acetanilide with known amount of carbon and nitrogen. Samples for POC analysis were previously acidified. The filters were encapsulated in a tin disk before analysis.

7

Culture conditions	Temperature (°C) controlled (incubator)	Salinity (psu) measured	Light period length (h) controlled (incubator)	Dark period length (h) controlled (incubator)	pH (total scale) adjusted	TA (µmol/kg) calculated (CO2sys)	DIC (µmol/kg) calculated (CO2sys)	CO_2 (µmol/kg) calculated (CO2sys)	HCO_3^- (µmol/kg) calculated (CO2sys)	CO_3^{2-} (µmol/kg) calculated (CO2sys)	pCO_2 (ppmv) initial target
1	15	33.86	14	10	8.29	2256.0	1913.6	7.51	1669.3	236.9	200
2	15	33.86	14	10	8.15	2275.0	2011.6	11.27	1813.9	186.5	300
3	15	33.86	14	10	8.04	2248.7	2042.2	15.03	1877.4	149.8	400
4	15	33.86	14	10	7.96	2272.4	2100.3	18.78	1951.9	129.6	500
5	15	33.86	14	10	7.89	2272.2	2128.8	22.54	1993.6	112.6	600
6	15	33.86	14	10	7.73	2269.0	2183.6	33.81	2068.9	80.9	900
7	15	33.86	14	10	7.61	2246.3	2199.7	45.08	2092.6	62.0	1200
8	15	33.86	14	10	7.55	2262.2	2233.8	52.59	2126.3	54.9	1400

Table 1: Experimental parameters of the mediums. The salinity has been measured in the initial medium. The temperature and the light and dark period length are controlled by incubator set up. The total alkalinity (TA) and the DIC, CO_2, HCO_3^- and CO_3^{2-} concentrations are calculated by CO2sys program. pCO_2 and pH correspond to the culture conditions tested.

210

# 3 Results

3.1 Physiological parameters and carbon content

3.1.1 Growth rates

The growth rates of the four strains do not show any statistical trend with changes in the carbonate chemistry of the medium
215 (*C. braarudii*: $r^2 = 0.04$ and $p > 0.05$, *H. carteri*: $r^2 = 0.08$ and $p > 0.05$, *G. oceanica*: $r^2 = 0.11$ and $p > 0.05$, *E. huxleyi*: $r^2 = 0.38$ and $p < 0.01$) (Figure 2). More than 85% of the data are comprised within a ±15% relative range of the mean growth rate for each strain (coloured band in Fig. 2). *E. huxleyi* and *G. oceanica* have the higher mean growth rate (0.87 d^{-1} and 0.67 d^{-1} respectively), while the larger *C. braarudii* and *H. carteri* have a mean growth rate of 0.58 d^{-1} and 0.24 d^{-1}, respectively (Figure 2). These absolute values are similar to those obtained in previous studies for *E. huxleyi*, *G. oceanica* and *C.*
220 *braarudii* (Phelps et al., 2021; Rickaby et al., 2010). *C. braarudii* has been reported with decreasing growth rates with rising CO_2 levels (Hermoso et al., 2016b; Rickaby et al., 2010).
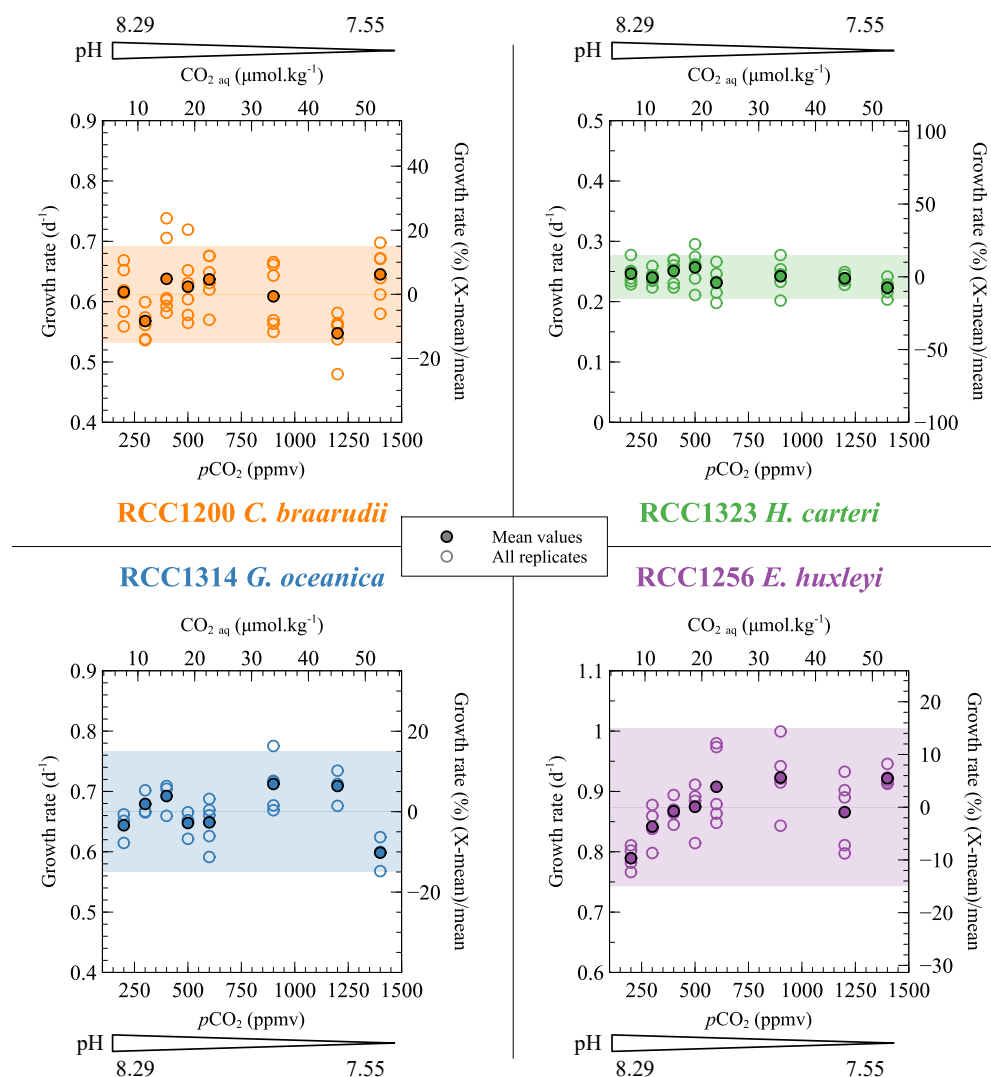
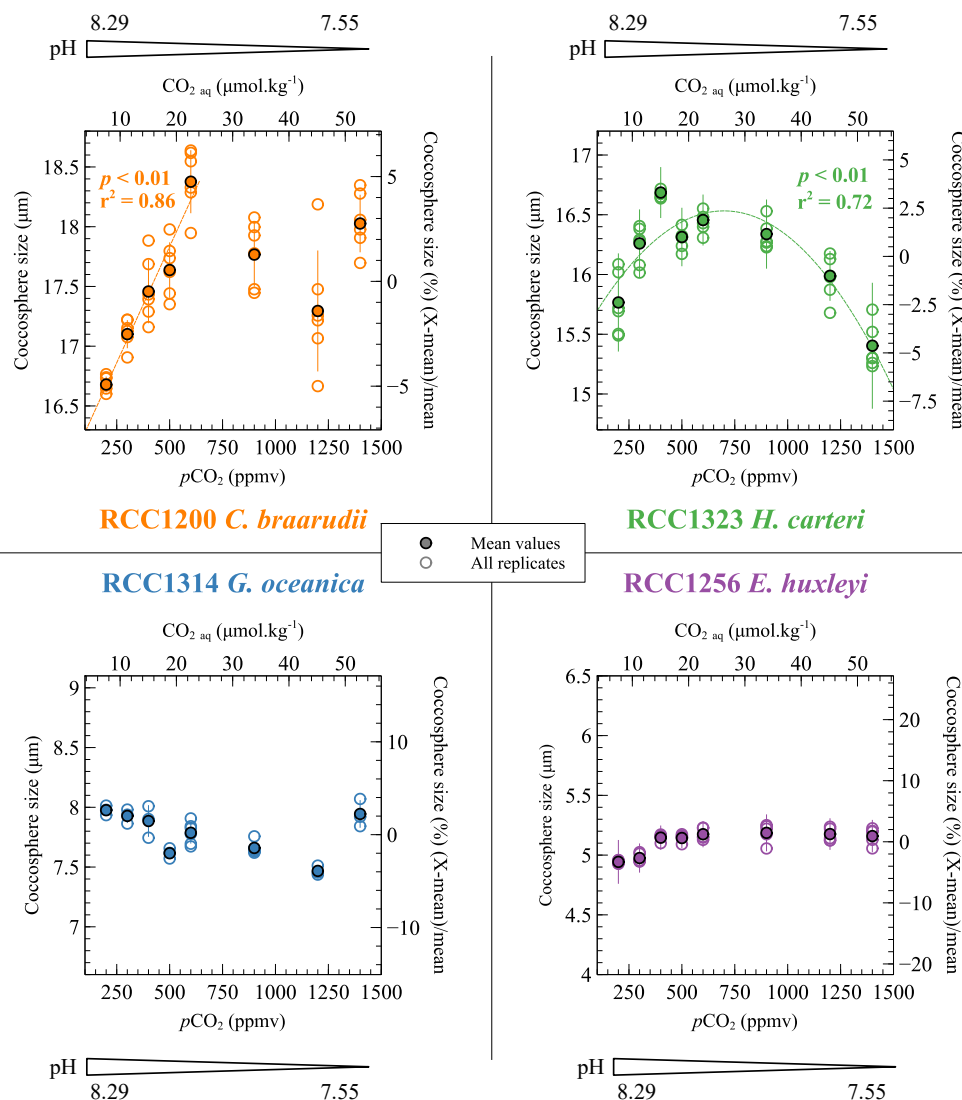**Figure 2: Specific growth rate (µ) of the four cultured strains with respect to CO_2 level and pH of the culture media. The empty dots show all the replicate data and the filled dots denote the mean growth rates. Growth rates are given in d^{-1} (left axis) and as a relative deviation of the mean growth rate of each strain (right axis). The coloured bands correspond to the range of ±15% of variation from the mean growth rate. More than 85% of the data are comprised within this range.**

3.1.2 Coccosphere sizes

The sizes of the coccospheres – i.e., the coccolithophore exoskeletons surrounding the cells, composed of coccoliths – approximate the evolution of cell size. The evolution of this parameter among the different strains varies with the CO_2/pH treatments. *C. braarudii* displays the largest coccospheres amongst the cultured strains. The mean coccosphere diameter of *C. braarudii* increases from 16.7 to 18.4 µm with increasing CO_2 levels from 200 to 600 ppmv and decreasing pH from 8.29

9

to 7.89 units of pH. The +1.70 µm increase in the coccosphere size represent a relative variation of 10.2% (r^2 = 0.86, p <

235   0.01). For higher pCO$_2$ and lower pH, the distribution of the coccosphere sizes is not linked with the carbonate chemistry (Figure 3). The size of *H. carteri* presents a hyperbolic trend (r^2 = 0.72, p < 0.01) of the coccosphere size with increasing CO$_2$ level and decreasing pH (+0.69 µm from 200 ppmv/8.29 pH units to 600 ppmv/7.89 pH units, and -1.05 µm from 600 ppmv/7.89 pH units to 1400 ppmv/7.55 pH units) (Figure 3). The size of the coccospheres produced by *G. oceanica* decreases from 8.0 to 7.5 µm with increasing CO$_2$ levels from 200 to 1200 ppmv and decreasing pH from 8.29 to 7.55 (-0.51

240   µm, a relative variation of 6.4%, r^2 = 0.67, p < 0.01) (Figure 3). The coccosphere size of the small species *E. huxleyi* exhibit a +0.22 µm increase with increasing pCO$_2$ and decreasing pH until 600 ppmv/7.89 pH units (a relative variation of 4.4%, r^2 = 0.77, p < 0.001). At higher pCO$_2$ and lower pH conditions, the coccosphere size is constant (r^2 = 0.04, p > 0.05) (Figure 3). These absolute values and trends in coccosphere size with changes in CO$_2$ level and pH are in line with previously reported coccosphere and cell sizes from previous culture studies (Hermoso, 2015; Hermoso et al., 2014, 2016b; Phelps et al., 2021;

245   Rickaby et al., 2010).

Figure 3: Evolution of the coccosphere sizes of the four cultured strains as a function of the CO_2 and pH culture conditions. The coccosphere sizes are given as the mean diameter of the coccospheres. They are given in µm (left axis) and as a percent relative to the mean coccosphere size of each strain (right axis). The empty points show the replicate data and the filled points show the mean coccosphere sizes.
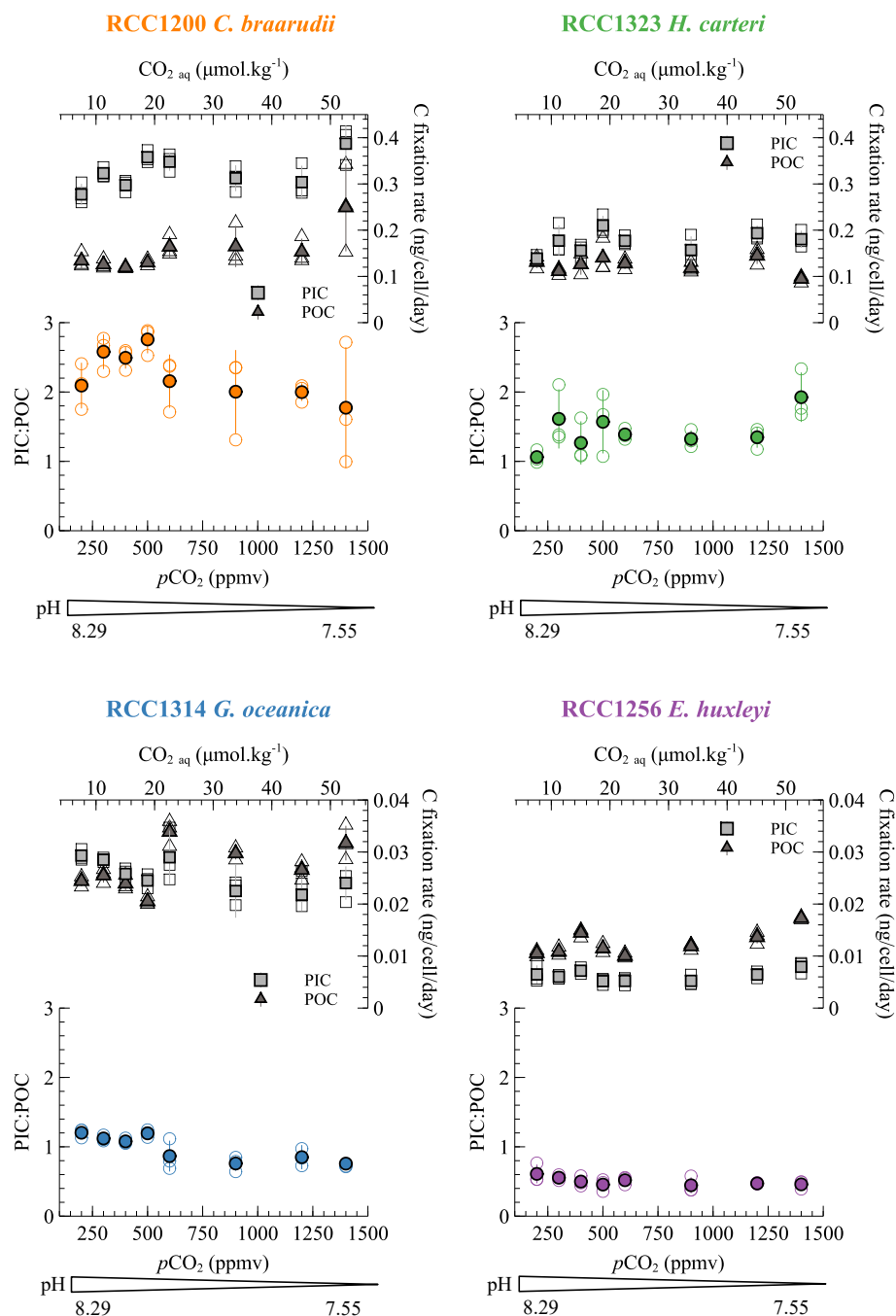
3.1.3 PIC:POC ratios

The PIC:POC ratio allows quantifying the respective allocation of carbon in its two fixation pathways (photosynthesis and calcification), which has isotopic implications on organic matter and coccoliths. The PIC:POC ratios of the four species do not show any statistically significant trend with changes in carbonate chemistry. Among the species cultured, *C. braarudii*

11

has the highest PIC:POC ratio (mean value of 2.23 ± 0.49), followed by *H. carteri* (mean value of 1.44 ± 0.35), *G. oceanica* (0.98 ± 0.20) and *E. huxleyi* (0.50 ± 0.09) (Figure 4). Those data are consistent with previously published PIC:POC data (Krug et al., 2011; Langer et al., 2006; Müller et al., 2010; Rickaby et al., 2010; Riebesell et al., 2000).
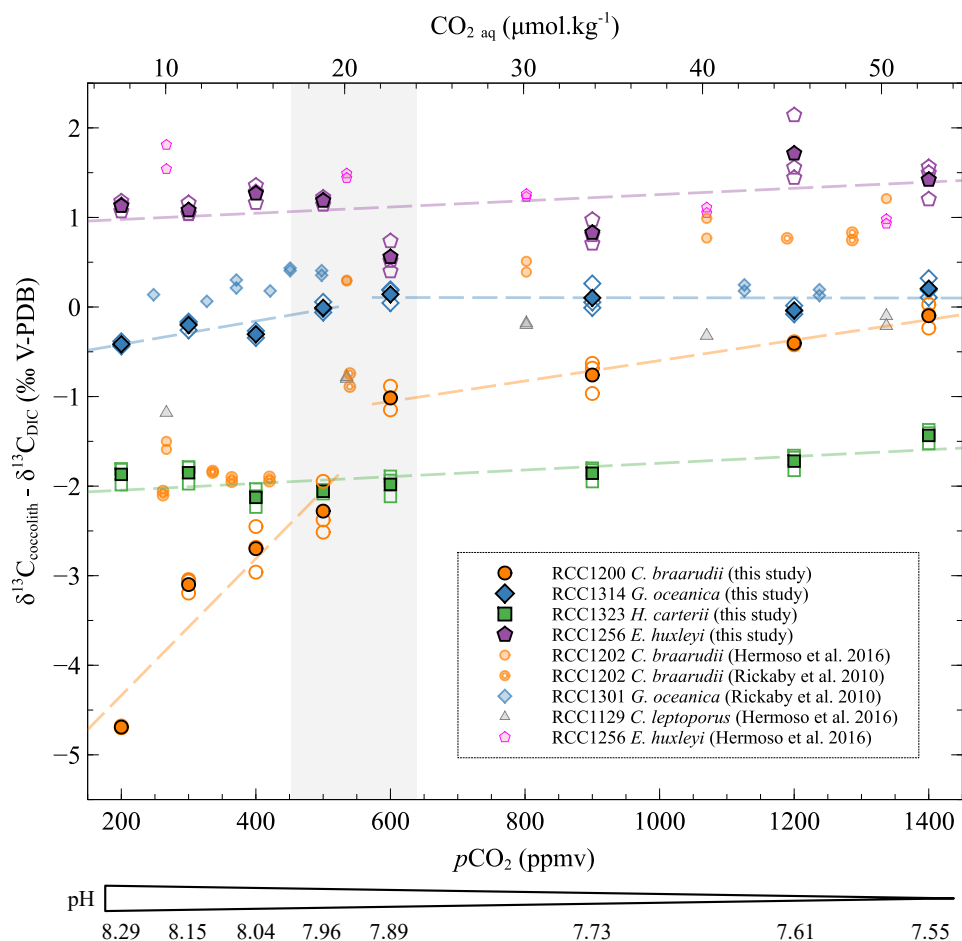
260

Figure 4: Particulate inorganic (square) and organic (triangle) carbon in ng per cell for each of the four species through the pCO_2 interval of the study (lower x-axis) and the aqueous CO_2 (upper x-axis). The PIC:POC ratios are also shown. The empty dots are all the replicate data and the filled points are the mean values for each species/condition.

265

3.2 Carbon isotope ratios of coccolith calcite

The species *E. huxleyi* does not show any significant trend in $\delta^{13}C_{coccolith}$ with changes in pCO_2 and pH ($r^2 = 0.16$, p > 0.05). The taxon *H. carteri* exhibits a minor increase of less than 0.5‰ in $\delta^{13}C_{coccolith}$ with increasing CO_2 level et decreasing pH ($r^2 = 0.49$, p < 0.001) (Figure 5). A key feature of the dataset pertains to the biogeochemical response of *C braarudii*. The

270 distribution of the isotope data with changes in carbonate chemistry can be divided into two distinct trends for *C. braarudii* and *G. oceanica*. The first trend corresponds to low CO_2 level from 200 to 500 ppmv and high pH from 8.29 to 7.96. The second stage corresponds to high CO_2 level from 600 to 1400 ppmv and low pH from 7.89 to 7.55 pH units. At low CO_2 levels and high pH, the $\delta^{13}C_{coccolith}$ of *C. braarudii* increases with increasing pCO_2 and decreasing pH (+2.41‰ V-PDB, a relative variation of 14%, $r^2 = 0.83$, p < 0.001). Regarding *G. oceanica*, it exhibits a small $\delta^{13}C_{coccolith}$ increase with

275 increasing pCO_2 and decreasing pH (+0.41‰ V-PDB, a relative variation of 3%, $r^2 = 0.61$, p < 0.01). Compared to low pCO_2 levels and high pH, the $\delta^{13}C_{coccolith}$ of *C. braarudii* increases with a less steep slope at high CO_2 levels and low pH (+0.92‰ V-PDB, a relative variation of 7%, $r^2 = 0.90$, p < 0.001). The $\delta^{13}C_{coccolith}$ of *G. oceanica* is steady at high pCO_2 and low pH ($r^2 = 0.10$, p > 0.05).

These $\delta^{13}C$ data do not exhibit any consistent trend with changes in growth rate, nor with PIC and POC. *G. oceanica* and *E.*

280 *huxleyi* show a carbon vital effect similar to that obtained in the work of Rickaby et al. (2010) and Hermoso et al. (2016). It is also similar to the dataset published in McClelland et al. (2017). The vital effects of *C. braarudii* in this study have a similar evolution with previously published results (Hermoso et al., 2016b; Rickaby et al., 2010) with a 1 ‰ shift towards more negative values (Figure 5).

Figure 5: Evolution of the carbon isotopic ratios of the four studied strains with increasing CO_2 concentration and decreasing pH. The data are represented as the $\delta^{13}C$ difference between coccoliths and DIC. The empty points are all the replicate data and the filled points are the means (circles: *Coccolithus braarudii*, RCC 1200; diamonds: *Gephyrocapsa oceanica*, RCC 1314; squares: *Helicosphaera carteri*; pentagons: *Emiliania huxleyi*). The grey band represents the carbonate chemistry condition where a shift in the carbon and oxygen isotope ratio occurs (between 500 and 600 ppmv). The pH indicated below only refers to the pH of the cultures of this study. The sources of previously reported data (smaller symbols) are inset.

3.3 Oxygen isotope ratios of coccolith calcite

The $\delta^{18}O_{coccolith}$ of *G. oceanica* is constant regardless ambiant conditions ($r^2 = 0.02$, $p > 0.05$), as for $\delta^{18}O_{coccolith}$ values of *E. huxleyi* ($r^2 = 0.15$, $p > 0.05$). The mean magnitude of the oxygen vital effects of *G. oceanica* and *E. huxleyi* are positive (+1.05‰ and +1.92‰, respectively), in good agreement with previously published data (Dudley et al., 1986; Hermoso et al., 2016b, a; Rickaby et al., 2010; Stevenson et al., 2014; Ziveri et al., 2003).

14

As already shown in the literature, *H. carteri* have a $\delta^{18}O_{coccolith}$ close to the inorganic reference (mean $\delta^{18}O_{coccolith}$ of +0.42‰) (Ziveri et al., 2003). Indeed, at low CO_2 concentrations and high pH, the $\delta^{18}O_{coccolith}$ of *H. carteri* is slowly

300 decreasing (-0.22‰, a relative variation of 4%, $r^2 = 0.57$, p < 0.01). From 600 ppmv and 7.89 pH units, the $\delta^{18}O_{coccolith}$ of *H. carteri* is stable ($r^2 \approx 0$, p > 0.05) (Figure 6).

The $\delta^{18}O_{coccolith}$ of *C. braarudii* is constant at low pCO_2 and high pH with a mean value of -0.81 ± 0.13‰ V-PDB and is also constant at high pCO_2 and low pH with a mean value of -0.37 ± 0.12‰ V-PDB. A significant difference in the *C. braarudii* $VE^{18}O$ is registered between high and low CO_2 ambient conditions in the culture medium. This +0.5‰ shift occurs between

305 500 and 600 ppmv. While we present evidence of a negative vital effect of coccoliths for *C. braarudii*, previous studies have shown a $\delta^{18}O_{coccolith}$ close to that of the inorganic for this species. (Hermoso, 2015; Hermoso et al., 2016a; Rickaby et al., 2010; Stevenson et al., 2014).
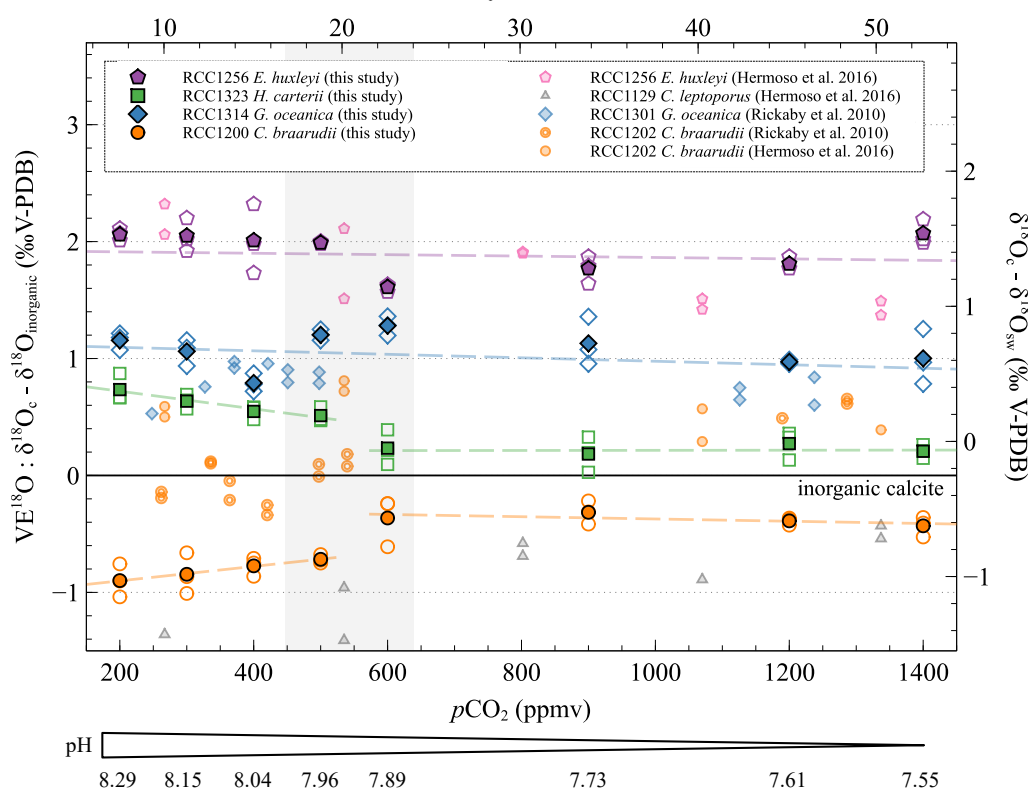

310 Figure 6: Evolution of the oxygen isotopic ratios of the four studied strains with increasing CO_2 concentration and decreasing pH. The data are represented as the vital effect (left axis) and as the isotopic difference between the seawater and the coccoliths $\delta^{18}O$ (right axis). The empty points are all the replicate data and the filled points are the means (circles: *Coccolithus braarudii*, RCC 1200; diamonds: *Gephyrocapsa oceanica*, RCC 1314; squares: *Helicosphaera carteri*; pentagons: *Emiliania huxleyi*). The vertical grey band represents the carbonate chemistry condition where a shift in the carbon and oxygen isotope ratio occurs. The black

315 line shows the calculated isotope ratio of an inorganic calcite (see Materials and methods). The pH scales indicated below only refers to the data published in this study. The sources of previously reported data (smaller symbols) are inset.

3.4 Carbon isotope ratios of organic matter

The carbon isotopic ratio of organic matter of *C. braarudii* is decreasing with increasing CO_2 level (from 200 to 500 ppmv)

320 and decreasing pH (from 8.29 to 7.89 pH units) ($r^2 = 0.93$, $p < 0.001$). This result is mirrored by a large $\delta^{13}C_{coccolith}$ increase (+2.4‰ V-PDB) (Figure 5). Above 600 ppmv (below 7.89 pH units), $\delta^{13}C_{org}$ of *C. braarudii* are stable and close to the values observed for the 200 ppmv/8.29 pH units condition (-30.77 ± 0.36‰ V-PDB) (Figure 7). $\delta^{13}C_{org}$ of *G. oceanica* do not change with changes in pCO$_2$ and pH (mean of -29.12 ± 0.41‰ V-PDB), similar to what was described for the changes in $\delta^{13}C_{coccolith}$.

325
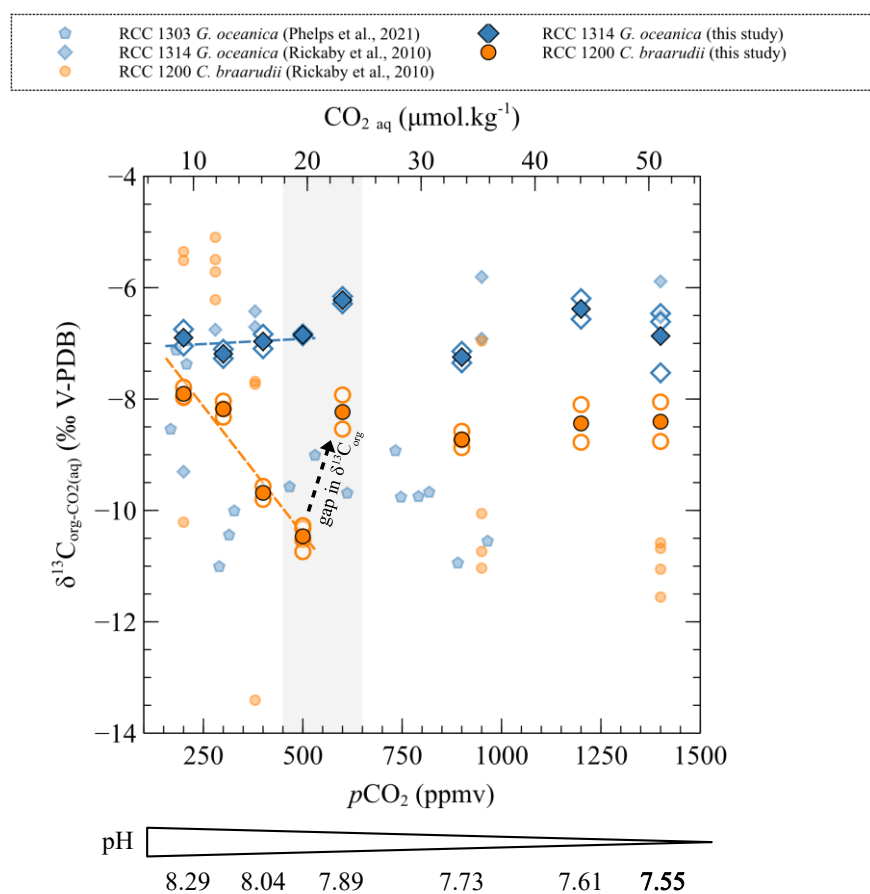
Figure 7: Carbon isotopic ratios of organic matter compared to $\delta^{13}C_{CO2\,aq}$ of the strains studied with changes in CO_2 level and pH. The empty points are all the replicate data and the filled points are the means. The grey band represents the carbonate chemistry condition where a shift in the carbon and oxygen isotope ratio occurs. The sources of previously reported data (smaller symbols)

330 **are inset.**

16

4 Discussion

The aim of our study is to quantify the environmental forcing exerted by CO_2 availability and ambient pH on the expression of vital effects of the coccolithophores with a view to develop and further palaeoenvironmental proxies. Our experimental results shed light onto the link between the environment, cellular growth and the efficiency of carbon fixation, as these parameters collectively control the expression of biologically-induced fractionation in organic and inorganic calcite. Published literature has revealed the role of carbon acquisition throughout the cell membrane and intracellular utilisation of carbon on the magnitude of the vital effect through laboratory and modelling studies (Laws et al., 1995; McClelland et al., 2017; Popp et al., 1998; Rau et al., 1996) Bolton and Stoll (2013) coined the concept of the demand-to-supply ratio to characterise the isotopic implication of carbon trafficking within the cells with large implication of the carbon isotope vital effect at different timescales. From these studies, it has emerged that the carbon isotopic composition of coccolith calcite was primarily controlled by the interplay of the inorganic carbon fixation in the coccolith vesicles and that of organic carbon in the chloroplast. At constant source of external carbon, the main driver dictating the $\delta^{13}C_{coccolith}$ is the amount and isotopic composition of organic matter produced through photosynthetic carbon fixation (POC/cell and $\delta^{13}C_{org}$ respectively) (McClelland et al., 2017).

As the foremost finding of our study, we show that *C. braarudii* exhibits a large $\delta^{13}C_{coccolith}$ increase (+2.4‰ V-PDB) mirrored by a $\delta^{13}C_{org}$ decrease (-2.6‰ V-PDB) from 200 ppmv and 8.29 pH units to 500 ppmv and 7.96 pH units (low pCO_2 and high pH conditions) (Figure 8). The correlation between $\delta^{13}C_{coccolith}$ and $\delta^{13}C_{org}$ of *C. braarudii* is not seen at high pCO_2 and low pH (600 to 1400 ppmv/7.89 to 7.55 pH units) (Figures 5 and 7). Based on this observation, we will treat separately the data obtained at low pCO_2/high pH from those obtained at high pCO_2/low pH in the following sections. It is also noteworthy that the small species *G. oceanica* and *E. huxleyi* do not show statistically-significant changes in $\delta^{13}C_{coccolith}$ nor $\delta^{13}C_{org}$ values coeval with changes in CO_2 level and pH (neither at low pCO_2 and high pH, nor over the whole interval).

4.1 The biogeochemical causes for the changes in $\delta^{13}C_{coccolith}$ of *C. braarudii* at low pCO_2 and high pH

Given that organic compounds are significantly ^{12}C-enriched relative to CO_2 with typical $\delta^{13}C_{org}$ values around –25‰, the more organic matter produced, the isotopically heavier the residual intracellular carbon pool. As calcification derives from this latter pool, coccoliths produced by highly photosynthetic coccolithophore cells exhibit relatively higher $\delta^{13}C$ values. This phenomenon is particularly expressed in small cells such as *E. huxleyi* and *G. oceanica* that are characterised by high POC contents and the highest $\delta^{13}C$ values (Ziveri et al., 2003) (Figures 4 and 5). We can hypothesise that a change in the efficiency of POC production with changes in carbon availability can induce a change in $\delta^{13}C_{coccolith}$ values, as it is apparent for *C. braarudii* with +2.4‰ V-PDB shift between low and high pCO_2 conditions (Figure 5). There is no apparent change in POC, PIC/POC or growth rates with the increase in $\delta^{13}C$ at low pCO_2 and high pH (Figures 2 and 4), despite an increase in

17

chlorophyll a concentration within the cells between 200 and 500 ppmv (Figure A2). These observations exclude a control of the amount of organic matter produced on the isotopic signature of the internal pool. Furthermore, a change in the efficiency of POC production could not explain the coeval -2.6‰ and progressive decrease in $\delta^{13}C_{org}$ values within this low pCO$_2$

365 interval. Thus, another biogeochemical process has to be sought.

A second means to explain coeval changes in both $\delta^{13}C_{org}$ and $\delta^{13}C_{coccolith}$ can rely on a change in the isotopic composition of the carbon acquired by the cell (CO$_2$ vs. HCO$_3^-$). Carbon concentrating mechanisms (Giordano et al., 2005) can induce a shift in internal carbon pool to which a contribution by HCO$_3^-$ ions by active transport becomes significant (Bolton and Stoll, 2013). Under this circumstance, the internal carbon may exhibit higher $\delta^{13}C$ values, as there is a typical 9‰ equilibrium

370 fractionation between CO$_2$ and HCO$_3^-$ (Zeebe and Wolf-Gladrow, 2001). However, early biological work aiming at characterising inducible CCMs in phytoplankton has revealed the lack of such active strategies of carbon acquisition in the large and ancestral *Coccolithus* taxon. Furthermore, the build-up of the carbon pool with a proportion of HCO$_3^-$ would have led to higher $\delta^{13}C$ values in both organic and inorganic pool, which is not what is observed at lowest pCO$_2$ (conversely, the $\delta^{13}C_{coccolith}$ values are lower) (Figures 5 and 7). These two lines of evidence rule out the CCM hypothesis.

375 The magnitude of carbon isotope fractionation between the CO$_2$ substrate and the organic matter is not constant and can change with the amount of ambient CO$_2$ forming the ground of the ε_{p-alk} proxy (Pagani, 2002; Popp et al., 1998). This modulation of the carbon kinetic fractionation by RuBisCO not only has consequences on the isotopic signature of the organic matter of which the compound-specific as alkenones, but also on the residual carbon pool, and ultimately on coccolith calcite.

380 Culture and wild coccolithophore data have revealed that the carbon isotope composition of the organic matter decreases with increasing CO$_2$ concentration (Bidigare et al., 1997). This biogeochemical control is compatible with the 2.6‰ decrease observed in $\delta^{13}C_{org}$ of *C. braarudii* between 200 and 500 ppmv (r² = 0.93, p < 0.001) (Figure 7). As the inorganic and organic carbon pool are linked at least from an isotopic perspective, we can interpret the +2.4‰ change in $\delta^{13}C_{coccolith}$ as the result of a modulation of kinetic fractionation of the organic matter via the increasing CO$_2$ availability (Figure 8).

385 As we do not observe any change in the growth rate nor in the POC per cell between low and high pCO$_2$ conditions, we suggest that the cells compensate for the decrease in carbon bioavailability in a different way. Indeed, the lower surface-to-volume ratio at 200 ppmv compared to 500 ppmv (cell diameter of 16.7 ±0.2 µm at 200 ppmv and 17.6 ±0.4 µm at 500 ppmv, in Fig. 3) may compensate for the lower supply with a lower demand to sustain growth rate (Bolton and Stoll, 2013; Rau et al., 1996).

390
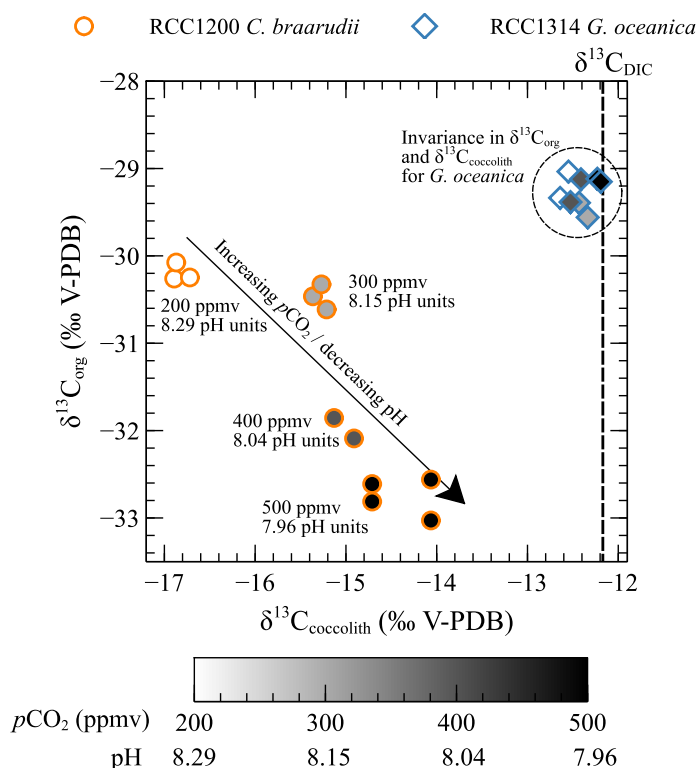
Figure 8: Scatter plot showing δ¹³Corg versus δ¹³Ccoccolith values with changes in *p*CO₂ and pH (circles: *Coccolithus braarudii*, RCC 1200; diamonds: *Gephyrocapsa oceanica*, RCC 1314). Grey levels correspond to growth conditions (white: 200 ppmv/8.29 pH units, light grey: 300 ppmv/8.15 pH units, dark grey: 400 ppmv/8.04 pH units, black: 500 ppmv/7.96 pH units).

395

4.2 Abrupt change in the isotope biogeochemistry of *Coccolithus braarudii* in response to alleviated carbon limitation and enhanced proton concentration in the cell

The data for *C. braarudii*, and in particular the link between CO_2 availability and the isotopic composition of coccoliths and organic matter, cannot be explained by a uniform biogeochemical framework, as a gap is seen for *C. braarudii* between 500

400 and 600 ppmv (Figures 5 and 7). The data show that above 600 ppmv, there is no correlation between ambient CO_2 levels and $\delta^{13}C_{org}$. Furthermore, there is no covariation between $\delta^{13}C_{org}$ and $\delta^{13}C_{coccolith}$ values of *C. braarudii* at high *p*CO_2 and low pH, in contrast to the covariation observed at low *p*CO_2 and high pH. The latter point suggests that the organic-to-inorganic forcing that occurs at low *p*CO_2 levels no longer operates at high *p*CO_2 levels. The fact that there is no organic-to-inorganic forcing at high *p*CO_2 is presumably due to the alleviation of carbon limitation, or at least due to a lower carbon demand-to-

405 supply ratio (Bolton et al., 2012). Likewise, coccosphere sizes exhibit no discernible trend with CO_2 concentrations at high CO_2 levels (Figure 3), in contrast to the findings at low CO_2 levels, which were tentatively attributed to a way to enhance CO_2 influx to the cells. This biogeochemical feature would indicate that the forcing of CO_2 availability on the apparent

$^{13}C/^{12}C$ fractionation between the organic matter and calcite occurs only below 600 ppmv. Meanwhile, small species (*E. huxleyi* and *G. oceanica*) show unchanged isotopic values with the pCO_2/pH treatments. As explained in Rickaby et al.

410 (2010) and Hermoso et al. (2016), the high surface to volume ratio of the small cells induces no carbon limitation at low CO_2 level, hence no impact of the change of pCO_2 and pH on the carbon isotopic system.

Elevated pCO_2 conditions are accompanied by greater proton concentrations in the environment (more acidic conditions). Calcifying phytoplankton such as the Coccolithophores has to efflux the excess protons generated by calcification by an active process operated by transmembrane Hv channels (Kottmeier et al., 2022; Taylor et al., 2011). Previous biological

415 studies have demonstrated that the opening of Hv channels are affected by intracellular pH (Taylor et al., 2011). Hv channels are closed at low pH to counter the influx of protons into the cell from the ambient environment. The pH threshold for the closure of the Hv channels has been assessed to be within the range of 8.1 – 7.5 pH units (Kottmeier et al., 2022). Therefore, assuming that the threshold stands between 7.96 and 7.89 pH units, the closure of the Hv channels is a good candidate for the 500-600 ppmv gap apparent in our dataset (Figures 5, 6 and 7). The closure of the Hv channels can thus result in an

420 accumulation of H^+ ions within the cytosol, leading to an intense decline in intracellular pH (Kottmeier et al., 2022; Taylor et al., 2011). The release of protons by coccolithogenesis is even more influential on intracellular pH for species such as *C. braarudii*, which produces a large amount of PIC compared to smaller cells (Figure 4). The latter cells (*G. oceanica* and *E. huxleyi*) indeed do not exhibit such a gap in $\delta^{13}C_{org}$ between 500 and 600 ppmv (small mean PIC values of 0.025 ±0.004 ng/cell and 0.006 ±0.001 ng/cell in the 600-1400 ppmv interval, respectively). Interestingly, the gap in *C. braarudii* $\delta^{13}C_{org}$

425 between low and high CO_2 levels is not seen in $\delta^{13}C_{coccolith}$. This observation could be the consequence of a decrease in the organic/inorganic carbon pool coupling when carbon supply is high, unlike bellow 500 ppmv when the small carbon pool imposes a high isotopic dependence between organic matter and calcite through Rayleigh distillation governed by the organic carbon fixation.

Around the same pCO_2/pH limit as presented for $\delta^{13}C_{coccolith}$ of *C. braarudii*, we observe a change in $\delta^{18}O_{coccolith}$ values. The

430 mean $VE^{18}O$ value is –0.81 ±0.13‰ V-PDB at low pCO_2/high pH conditions, while the mean $VE^{18}O$ value is –0.37 ±0.12‰ V-PDB at high pCO_2/low pH conditions (Figure 6). The gap in $\delta^{18}O_{coccolith}$ can be explained by the change in pH. When the pH in the environment is low, it has been demonstrated that the $^{18}O/^{16}O$ equilibration time between DIC species and H_2O is shorter compared to high pH conditions (Usdowski et al., 1991). The isotopic equilibration between $\delta^{18}O_{DIC}$ and $\delta^{18}O_{sw}$ due to the assimilation of isotopically heavy CO_2 into the cell is consequently more complete at low pH than at high pH. As a

435 consequence, $\delta^{18}O_{DIC}$ (and consequently $\delta^{18}O_{coccolith}$) values are closer to $\delta^{18}O_{sw}$ at high pCO_2 and low pH (Figure 6). The $\delta^{18}O_{coccolith}$ difference between high and low pH levels is consistent with a change in pH homeostasis strategy between 7.96 and 7.89 pH units that can be responsible for the $\delta^{13}C$ before and after 500/600 ppmv.

4.3 Palaeoclimatic implications of the CO_2 proxy based on $\delta^{13}C_{coccolith}$

440 ### 4.3.1 $\Delta\delta^{13}C_{small-large}$ evolution with changes in CO_2 levels and pH

The increase in $\delta^{13}C_{coccolith}$ of *C. braarudii* with rising pCO_2 and decreasing pH shows potential as a proxy for reconstructing past carbonate chemistry, and consequently atmospheric pCO_2. However, utilizing absolute carbon vital effects of coccoliths for palaeo-pCO_2 reconstructions requires accurate knowledge of the $\delta^{13}C_{inorganic}$ (DIC) of past oceans, which remains challenging (Hermoso et al., 2020). To overcome this issue, previous studies (Bolton et al., 2012; Bolton and Stoll, 2013;

445 Godbillot et al., 2022; Hermoso et al., 2016b; McClelland et al., 2017; Tremblin et al., 2016) have proposed the use of the offset between the $\delta^{13}C_{coccolith}$ of small and large species, known as the differential vital effect (noted $\Delta\delta^{13}C$, Eq. (3)). Indeed, the $\delta^{13}C_{coccolith}$ of the small cells (Noelaerhabdaceae) is steady regardless of the pCO_2 levels due to their relatively large carbon pool, akin to *C. braarudii* under carbon replete conditions (at high pCO_2 and low pH). The coccolith-based palaeo-pCO_2 proxy is independent of the isotope ratio of ambient DIC, as both small and large coccoliths are produced by cells

450 growing in the same shallow water. In practical terms, $\Delta\delta^{13}C_{small-large}$ can be expressed as follows:

$$\Delta\delta^{13}C_{small-large} = \delta^{13}C_{small\ coccolith} - \delta^{13}C_{large\ coccolith} \ , \tag{3}$$

where $\delta^{13}C$ is expressed in ‰ V-PDB. The small coccoliths used in this work are those of *G. oceanica* and the large coccoliths are those of *C. braarudii*.

$\Delta\delta^{13}C$ and pCO_2 data highlight a linear relationship across the range of 200 to 500 ppmv (i.e., pH values between 8.29 and

455 7.96), that we previously explained by a modulation in the carbon isotope fractionation between $CO_{2\ aq}$ and the organic matter (Figure 9, Equation (4)). The uncertainties associated with the constants in Eq. (4) represent the standard deviation obtained with a linear regression model.

$$CO_{2\ aq}(\pm3.17) = -4.65(\pm0.72) \times \Delta\delta^{13}C_{G.\ oceanica - C.\ braarudii} + 26.90(\pm2.21) \ , \tag{4}$$

where $CO_{2\ aq}$ is expressed in µmol.kg^{-1} and $\Delta\delta^{13}C$ is expressed in ‰ V-PDB.

460
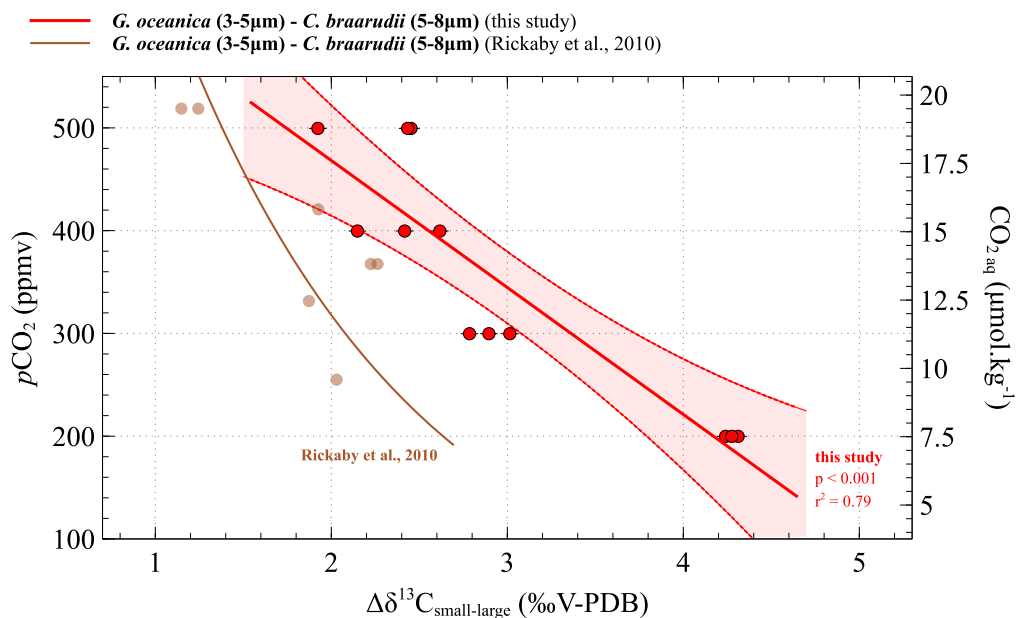
Figure 9: Calibration between CO_2 and $\Delta\delta^{13}C_{small-large}$ obtained from culture experiments. The results of our study are shown in red (replicate data as dots, the linear regression made between 200 and 500 ppmv corresponds to the solid line and the confidence interval is shown with dotted lines). The brown curve is the equation recalculated from Rickaby et al. (2010) dataset. The relation encompassing the 200-1400 ppmv spectrum is shown in Figure A1.

4.3.2 Palaeoclimate application of carbon isotope culture data

In this study, we refine a geological CO_2-sensitive probe by the use of the $\Delta\delta^{13}C_{small-large}$ isotopic offset. This probe forms the basis for a palaeo-CO_2 proxy transferable to sedimentary records from geological periods with low CO_2 levels, such as the Neogene and the Quaternary (Bolton and Stoll, 2013; Godbillot et al., 2022; Hermoso et al., 2020). Providing a new palaeo-pCO_2 proxy for those periods is of key interest, as it has been shown that alkenones are less sensitive to low and medium CO_2 level changes (Badger et al., 2019). Another strength of the pCO_2 proxy presented here is that it is based on coccolith calcite, which can be separated from other sedimentary components according to their size ranges by microfiltering and centrifuging protocols (Minoletti et al., 2008; Stoll and Ziveri, 2002; Zhang et al., 2018, 2021).

In addition, our study provides a biogeochemical explanation for $\Delta\delta^{13}C_{small-large}$ changes with CO_2 level and pH, thus supporting the reliability of these equations for palaeoclimate applications. We also demonstrate that the $\Delta\delta^{13}C_{small-large}$-$CO_2$ calibration can be extended to the whole interval studied, i.e., above 600 ppmv (Figure A1). Despite the fact that the link between $\Delta\delta^{13}C_{small-large}$ and CO_2 levels is less constrained and understood at high CO_2 level than at low CO_2 levels, the relationship is statistically supported on the whole interval ($r^2 = 0.80$, $p < 0.001$) (Figure A1). Thus, this calibration can potentially be used to reconstruct palaeo-CO_2 levels throughout the entire Cenozoic era.

5 Conclusion

The combined study of the impact of CO_2 concentration and pH on the fractionation of carbon and oxygen isotopes in coccolithophores (in their organic matter and calcite biominerals) provides an explanation of the cause of variations in $\Delta\delta^{13}C_{small-large}$. One of the major findings of this study is the coeval variation of $\delta^{13}C_{coccolith}$ and $\delta^{13}C_{org}$ in *Coccolithus braarudii* with changes in pCO_2 between 200 and 500 ppmv and pH between 8.29 and 7.96. Combined with the fact that physiological parameters (growth rates, PIC, and POC) of *C. braarudii* remain unchanged despite changes in the availability of carbon, these results indicate that the cause of variations in $\delta^{13}C_{coccolith}$ is an environmental-driven change in the magnitude of the fractionation between ambient $CO_{2\ aq}$ and organic matter produced by *C. braarudii*. Above 500 ppmv, and for pH values below 7.96, greater carbon availability induces isotopic decoupling between $\delta^{13}C_{org}$ and $\delta^{13}C_{coccolith}$. On the other hand, small species exhibit no change in $\delta^{13}C_{coccolith}$ or $\delta^{13}C_{org}$ in response to changes in CO_2 levels and pH. By comparing $\delta^{13}C_{coccolith}$ of small (*G. oceanica* or *E. huxleyi*) with those of large cells (*C. braarudii*), we have established an insightful $\Delta\delta^{13}C$-CO_2 transfer equation relevant for the Neogene and Quaternary timeslices.

## Appendices
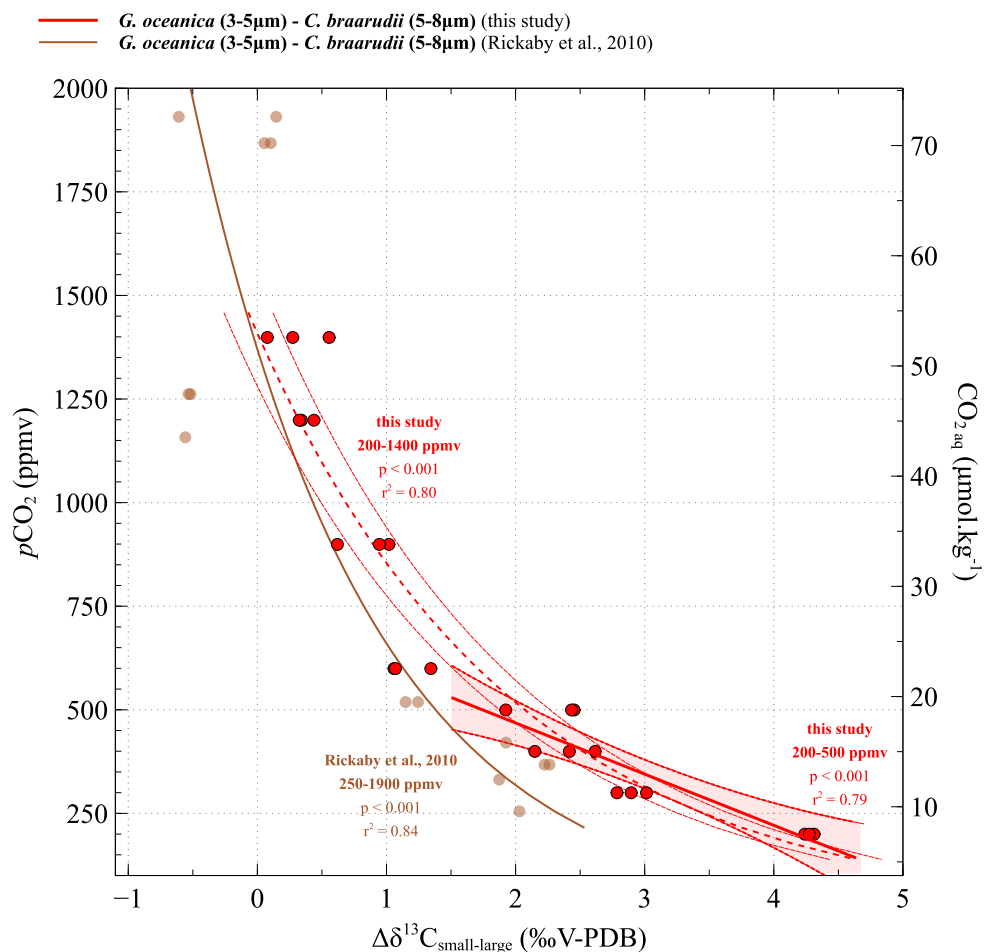
Figure A1: Calibration between CO₂ concentrations and Δδ¹³C_small-large obtained from culture experiments at low and high CO₂ levels. The results of our study are shown in red. Replicate data are illustrated with red dots. The linear regression made between 200 and 500 ppmv corresponds to the solid line and the confidence interval is shown with dotted lines. The dotted line shows the logarithmic regression made for the data on the whole interval (200 to 500 ppmv). The brown curve is the equation recalculated from Rickaby et al. (2010) dataset.
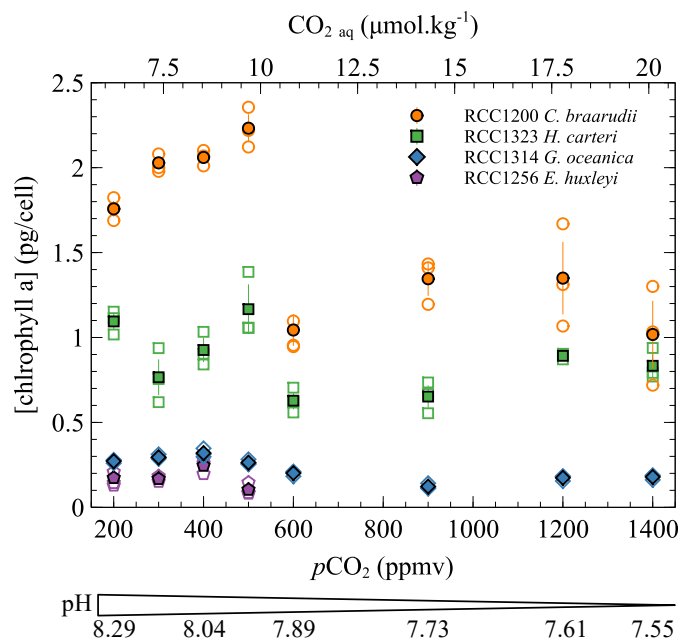
Figure A2: Chlorophyll a concentration (pg/cell) as a function of CO_2 and pH. The empty points are all the replicate data and the filled points are the means (circles: *Coccolithus braarudii*, RCC 1200; diamonds: *Gephyrocapsa oceanica*, RCC 1314; squares: *Helicosphaera carteri*; pentagons: *Emiliania huxleyi*). Measurements of chlorophyll a concentration were conducted using fluorometry according to the SOMLIT national protocol (Yentsch and Menzel, 1963)**. A Turner Design Trilogy fluorometer was employed to measure the fluorescence of our samples before and after acidification. The samples were acidified with 10 µL of hydrochloric acid per ml of acetone extract and left in the dark for 2 minutes between the two measurements. The equation used to calculate the chlorophyll concentration is as follows** (Lorenzen, 1967)**.**

Data availability:

All numerical data generated in this study are included in the Supplement.

Supplement:

The data related to this article will be available online upon publication at: https://doi.org/10.5281/zenodo.12187457

Author contributions:

This study was conceived by MH and FM. Experiments were undertaken by GLG, CG and MH. Measurements were done by GLG, CG, GD and VR. Data were analysed by GLG, MH and FM. The paper was written by GLG, FM and MH with inputs from the other authors.

Competing interests:

The authors declare that they have no conflict of interest.

530 **References**

Bach, L. T., MacKinder, L. C. M., Schulz, K. G., Wheeler, G., Schroeder, D. C., Brownlee, C., and Riebesell, U.: Dissecting the impact of CO_2 and pH on the mechanisms of photosynthesis and calcification in the coccolithophore Emiliania huxleyi, New Phytologist, 199, 121–134, https://doi.org/10.1111/nph.12225, 2013.

Badger, M. P. S., Chalk, T. B., Foster, G. L., Bown, P. R., Gibbs, S. J., Sexton, P. F., Schmidt, D. N., Pälike, H., Mackensen,
535 A., and Pancost, R. D.: Insensitivity of alkenone carbon isotopes to atmospheric CO_2 at low to moderate CO_2 levels, Climate of the Past, 15, 539–554, https://doi.org/10.5194/cp-15-539-2019, 2019.

Bakker, D. C. E., Pfeil, B., Landa, C. S., Metzl, N., O'Brien, K. M., Olsen, A., Smith, K., Cosca, C., Harasawa, S., Jones, S. D., Nakaoka, S. I., Nojiri, Y., Schuster, U., Steinhoff, T., Sweeney, C., Takahashi, T., Tilbrook, B., Wada, C., Wanninkhof, R., Alin, S. R., Balestrini, C. F., Barbero, L., Bates, N. R., Bianchi, A. A., Bonou, F., Boutin, J., Bozec, Y., Burger, E. F.,
540 Cai, W. J., Castle, R. D., Chen, L., Chierici, M., Currie, K., Evans, W., Featherstone, C., Feely, R. A., Fransson, A., Goyet, C., Greenwood, N., Gregor, L., Hankin, S., Hardman-Mountford, N. J., Harlay, J., Hauck, J., Hoppema, M., Humphreys, M. P., Hunt, C. W., Huss, B., Ibánhez, J. S. P., Johannessen, T., Keeling, R., Kitidis, V., Körtzinger, A., Kozyr, A., Krasakopoulou, E., Kuwata, A., Landschützer, P., Lauvset, S. K., Lefèvre, N., Lo Monaco, C., Manke, A., Mathis, J. T., Merlivat, L., Millero, F. J., Monteiro, P. M. S., Munro, D. R., Murata, A., Newberger, T., Omar, A. M., Ono, T., Paterson,
545 K., Pearce, D., Pierrot, D., Robbins, L. L., Saito, S., Salisbury, J., Schlitzer, R., Schneider, B., Schweitzer, R., Sieger, R., Skjelvan, I., Sullivan, K. F., Sutherland, S. C., Sutton, A. J., Tadokoro, K., Telszewski, M., Tuma, M., Van Heuven, S. M. A.

C., Vandemark, D., Ward, B., Watson, A. J., and Xu, S.: A multi-decade record of high-quality fCO2 data in version 3 of the Surface Ocean CO2 Atlas (SOCAT), https://doi.org/10.5194/essd-8-383-2016, 15 September 2016.

Berges, J. A., Franklin, D. J., and Harrison, P. J.: Evolution of an artificial seawater medium: Improvements in enriched
550   seawater, artificial water over the last two decades, J Phycol, 37, 1138–1145, https://doi.org/10.1046/j.1529-8817.2001.01052.x, 2001.

Bidigare, R., Freeman, H., Hanson, L., Hayes, M., Jasper, P., King, L., Millero, J., Popp, N., Steinberg, A., and Wakeham, G.: Consistent fractionation of 13C in nature and in the laboratory: Growth-rate effects in some haptophyte algae, Global Biogeochem Cycles, 11, 279–292, 1997.

555   Bolton, C. T. and Stoll, H. M.: Late Miocene threshold response of marine algae to carbon dioxide limitation, Nature, 500, 558–562, https://doi.org/10.1038/nature12448, 2013.

Bolton, C. T., Stoll, H. M., and Mendez-Vicente, A.: Vital effects in coccolith calcite: Cenozoic climate- pCO2 drove the diversity of carbon acquisition strategies in coccolithophores?, Paleoceanography, 27, https://doi.org/10.1029/2012PA002339, 2012.

560   Claxton, L. M., McClelland, H. L. O., Hermoso, M., and Rickaby, R. E. M.: Eocene emergence of highly calcifying coccolithophores despite declining atmospheric CO2, Nat Geosci, 2, https://doi.org/10.1038/s41561-022-01006-0, 2022.

Dudley, W. C., Blackwelder, P., Brand, L., and Duplessy, J. C.: Stable isotopic composition of coccoliths, Mar Micropaleontol, 10, 1–8, https://doi.org/10.1016/0377-8398(86)90021-6, 1986.

Ellis, R. J.: The most abundant protein in the world, Trends Biochem Sci, 4, 241–244, https://doi.org/10.1016/0968-
565   0004(79)90212-3, 1979.

Foster, G. L.: Seawater pH, pCO2 and [CO2-3] variations in the Caribbean Sea over the last 130 kyr: A boron isotope and B/Ca study of planktic foraminifera, Earth Planet Sci Lett, 271, 254–266, https://doi.org/10.1016/j.epsl.2008.04.015, 2008.

Giordano, M., Beardall, J., and Raven, J. A.: CO2 concentrating mechanisms in algae: Mechanisms, environmental modulation, and evolution, Annu Rev Plant Biol, 56, 99–131, https://doi.org/10.1146/annurev.arplant.56.032604.144052,
570   2005.

Godbillot, C., Minoletti, F., Bassinot, F., and Hermoso, M.: Parallel between the isotopic composition of coccolith calcite and carbon levels across Termination II: developing a new paleo-CO2 probe, Climate of the Past, 18, 449–464, https://doi.org/10.5194/cp-18-449-2022, 2022.

Gutknecht, J., Bisson, M. A., and Tosteson, F. C.: Diffusion of carbon dioxide through lipid bilayer membranes: effects of
575   carbonic anhydrase, bicarbonate, and unstirred layers., J Gen Physiol, 69, 779–794, https://doi.org/10.1085/jgp.69.6.779, 1977.

Guy, R. D., Fogel, M. L., and Berry, J. A.: Photosynthetic fractionation of the stable isotopes of oxygen and carbon, Plant Physiol, 101, 37–47, https://doi.org/10.1104/pp.101.1.37, 1993.

Hermoso, M.: Control of ambient pH on growth and stable isotopes in phytoplanktonic calcifying algae, Paleoceanography,
580   30, 1100–1112, https://doi.org/10.1002/2015PA002844, 2015.

Hermoso, M., Horner, T. J., Minoletti, F., and Rickaby, R. E. M.: Constraints on the vital effect in coccolithophore and dinoflagellate calcite by oxygen isotopic modification of seawater, Geochim Cosmochim Acta, 141, 612–627, https://doi.org/10.1016/j.gca.2014.05.002, 2014.

585   Hermoso, M., Minoletti, F., Aloisi, G., Bonifacie, M., McClelland, H. L. O., Labourdette, N., Renforth, P., Chaduteau, C., and Rickaby, R. E. M.: An explanation for the 18O excess in Noelaerhabdaceae coccolith calcite, Geochim Cosmochim Acta, 189, 132–142, https://doi.org/10.1016/j.gca.2016.06.016, 2016a.

Hermoso, M., Chan, I. Z. X., McClelland, H. L. O., Heureux, A. M. C., and Rickaby, R. E. M.: Vanishing coccolith vital effects with alleviated carbon limitation, Biogeosciences, 13, 301–312, https://doi.org/10.5194/bg-13-301-2016, 2016b.

Hermoso, M., McClelland, H. L. O., Hirst, J. S., Minoletti, F., Bonifacie, M., and Rickaby, R. E. M.: Towards the use of the
590   coccolith vital effects in palaeoceanography: A field investigation during the middle Miocene in the SW Pacific Ocean, Deep Sea Res 1 Oceanogr Res Pap, 160, https://doi.org/10.1016/j.dsr.2020.103262, 2020.

Jasper, J. P. and Hayes, J. M.: A carbon isotope record of CO2 levels during the late Quaternary, Nature, 347, 462–464, https://doi.org/10.1038/347462a0, 1990.

Keller, M. D., Selvin, R. C., Claus, W., and Guillard, R. R. L.: Media for the culture of oceanic ultraphytoplankton, J Phycol,
595   23, 633–638, https://doi.org/10.1111/j.1529-8817.1987.tb04217.x, 1987.

Klochko, K., Kaufman, A. J., Yao, W., Byrne, R. H., and Tossell, J. A.: Experimental measurement of boron isotope fractionation in seawater, Earth Planet Sci Lett, 248, 276–285, https://doi.org/10.1016/j.epsl.2006.05.034, 2006.

Kottmeier, D. M., Chrachri, A., Langer, G., Helliwell, K. E., Wheeler, G. L., and Brownlee, C.: Reduced H + channel activity disrupts pH homeostasis and calcification in coccolithophores at low ocean pH, https://doi.org/10.1073/pnas, 2022.

600   Krug, S. A., Schulz, K. G., and Riebesell, U.: Effects of changes in carbonate chemistry speciation on Coccolithus braarudii: A discussion of coccolithophorid sensitivities, Biogeosciences, 8, 771–777, https://doi.org/10.5194/bg-8-771-2011, 2011.

Langer, G., Geisen, M., Baumann, K. H., Kläs, J., Riebesell, U., Thoms, S., and Young, J. R.: Species-specific responses of calcifying algae to changing seawater carbonate chemistry, Geochemistry, Geophysics, Geosystems, 7, https://doi.org/10.1029/2005GC001227, 2006.

605   Laws, E. A., Popp, B. N., Bidigare, R. R., Kennicutt, M. C., and Macko, S. A.: Dependence of phytoplankton carbon isotopic composition on growth rate and [CO2]aq: Theoretical considerations and experimental results, Geochim Cosmochim Acta, 59, 1131–1138, 1995.

Laws, E. A., Popp, B. N., Bidigare, R. R., Riebesell, U., Burkhardt, S., and Wakeham, S. G.: Controls on the molecular distribution and carbon isotopic composition of alkenones in certain haptophyte algae, Geochemistry, Geophysics,
610   Geosystems, 2, https://doi.org/10.1029/2000gc000057, 2001.

Lorenzen, C. J.: Determination of chlorophyll and pheo-pigments: spectrophotometric equations, Limnol Oceanogr, 12, 343–346, https://doi.org/10.4319/lo.1967.12.2.0343, 1967.

McClelland, H. L. O., Bruggeman, J., Hermoso, M., and Rickaby, R. E. M.: The origin of carbon isotope vital effects in coccolith calcite, Nat Commun, 8, https://doi.org/10.1038/ncomms14511, 2017.

615   Minoletti, F., Hermoso, M., and Gressier, V.: Separation of sedimentary micron-sized particles for palaeoceanography and calcareous nannoplankton biogeochemistry, Nat Protoc, 4, 14–24, https://doi.org/10.1038/nprot.2008.200, 2008.

Müller, M. N., Schulz, K. G., and Riebesell, U.: Effects of long-term high CO_2 exposure on two species of coccolithophores, Biogeosciences, 7, 1109–1116, https://doi.org/10.5194/bg-7-1109-2010, 2010.

Pagani, M.: The alkenone - CO_2 proxy and ancient atmospheric carbon dioxide, Philosophical Transactions of the Royal

620   Society A: Mathematical, Physical and Engineering Sciences, 360, 609–632, https://doi.org/10.1098/rsta.2001.0959, 2002.

Pagani, M., Arthur, M. A., and Freeman, K. H.: Miocene evolution of atmospheric carbon dioxide, Paleoceanography, 14, 273–292, https://doi.org/10.1029/1999PA900006, 1999.

Pagani, M., Liu, Z., LaRiviere, J., and Ravelo, A. C.: High Earth-system climate sensitivity determined from Pliocene carbon dioxide concentrations, Nat Geosci, 3, 27–30, https://doi.org/10.1038/ngeo724, 2010.

625   Parker, M. D. and Boron, W. F.: The Divergence, Actions, Roles, and Relatives of Sodium-Coupled Bicarbonate Transporters, Physiol Rev, 93, 803–959, https://doi.org/10.1152/physrev.00023.2012, 2013.

Phelps, S. R., Hennon, G. M. M., Dyhrman, S. T., Hernández Limón, M. D., Williamson, O. M., and Polissar, P. J.: Carbon Isotope Fractionation in Noelaerhabdaceae Algae in Culture and a Critical Evaluation of the Alkenone Paleobarometer, Geochemistry, Geophysics, Geosystems, 22, 1–20, https://doi.org/10.1029/2021GC009657, 2021.

630   Popp, B. N., Laws, E. A., Bidigare, R. R., Dore, J. E., Hanson, K. L., and Wakeham, S. G.: Effect of Phytoplankton Cell Geometry on Carbon Isotopic Fractionation, Geochim Cosmochim Acta, 62, 69–77, https://doi.org/10.1016/S0016-7037(97)00333-5, 1998.

Rae, J. W. B., Zhang, Y. G., Liu, X., Foster, G. L., Stoll, H. M., and Whiteford, R. D. M.: Atmospheric CO_2 over the Past 66 Million Years from Marine Archives, Annu Rev Earth Planet Sci, 49, 609–641, https://doi.org/10.1146/annurev-earth-

635   082420-063026, 2021.

Rau, G. H., Riebesell, U., and Wolf-Gladrow, D.: A model of photosynthetic 13C fractionation by marine phytoplankton based on diffusive molecular CO_2 uptake, Mar Ecol Prog Ser, 133, 275–285, https://doi.org/10.3354/meps133275, 1996.

Reinfelder, J. R.: Carbon concentrating mechanisms in eukaryotic marine phytoplankton, Ann Rev Mar Sci, 3, 291–315, https://doi.org/10.1146/annurev-marine-120709-142720, 2011.

640   Rickaby, R. E. M., Henderiks, J., and Young, J. N.: Perturbing phytoplankton: Response and isotopic fractionation with changing carbonate chemistry in two coccolithophore species, Climate of the Past, 6, 771–785, https://doi.org/10.5194/cp-6-771-2010, 2010.

Riebesell, U., Zondervan, I., Rost, B., Tortell, P. D., Zeebe, R. E., and Morel, F. M. M.: Reduced calcification of marine plankton in response to increased atmospheric CO_2, Nature, 407, 364–367, https://doi.org/10.1038/35030078, 2000.

645   Romero, M. F., Fulton, C. M., and Boron, W. F.: The SLC4 family of HCO_3- transporters, Pflugers Arch, 447, 495–509, https://doi.org/10.1007/s00424-003-1180-2, 2004.

Sanyal, A., Hemming, N. G., Hanson, G. N., and Broecker, W. S.: Evidence for a higher pH in the glacial ocean from boron isotopes in foraminifera, Nature, 373, 234–236, https://doi.org/10.1038/373234a0, 1995.

Sosdian, S. M., Greenop, R., Hain, M. P., Foster, G. L., Pearson, P. N., and Lear, C. H.: Constraining the evolution of
650   Neogene ocean carbonate chemistry using the boron isotope pH proxy, Earth Planet Sci Lett, 498, 362–376, https://doi.org/10.1016/j.epsl.2018.06.017, 2018.

Stevenson, E. I., Hermoso, M., Rickaby, R. E. M., Tyler, J. J., Minoletti, F., Parkinson, I. J., Mokadem, F., and Burton, K. W.: Controls on stable strontium isotope fractionation in coccolithophores with implications for the marine Sr cycle, Geochim Cosmochim Acta, 128, 225–235, https://doi.org/10.1016/j.gca.2013.11.043, 2014.

655   Stoll, H. M. and Ziveri, P.: Separation of monospecific and restricted coccolith assemblages from sediments using differential settling velocity, Mar Micropaleontol, 46, 209–221, https://doi.org/10.1016/S0377-8398(02)00040-3, 2002.

Taylor, A. R., Chrachri, A., Wheeler, G., Goddard, H., and Brownlee, C.: A voltage-gated H+ channel underlying pH homeostasis in calcifying Coccolithophores, PLoS Biol, 9, https://doi.org/10.1371/journal.pbio.1001085, 2011.

Tremblin, M., Hermoso, M., and Minoletti, F.: Equatorial heat accumulation as a long-term trigger of permanent Antarctic
660   ice sheets during the Cenozoic, Proceedings of the National Academy of Sciences, 113, 11782–11787, https://doi.org/10.1073/pnas.1608100113, 2016.

Tripati, A. K., Roberts, C. D., Eagle, R. A., and Li, G.: A 20 million year record of planktic foraminiferal B/Ca ratios: Systematics and uncertainties in pCO2 reconstructions, Geochim Cosmochim Acta, 75, 2582–2610, https://doi.org/10.1016/j.gca.2011.01.018, 2011.

665   Usdowski, E., Michaelis, J., Bottcher, M. E., and Hoef, J.: Factors for the oxygen isotope equilibrium fractionation between aqueous and gaseous CO_2, carbonic acid, bicarbonate, carbonate, and water (19°C), Zeitschrift für Physikalische Chemie, 170, 237–249, 1991.

Wolf-Gladrow, D. and Riebesell, U.: Diffusion and reactions in the vicinity of plankton: A refined model for inorganic carbon transport, Mar Chem, 59, 17–34, https://doi.org/10.1016/S0304-4203(97)00069-8, 1997.

670   Yentsch, C. S. and Menzel, D. W.: A method for the determination of phytoplankton chlorophyll and phaeophytin by fluorescence, Deep-Sea Research and Oceanographic Abstracts, 10, 221–231, https://doi.org/10.1016/0011-7471(63)90358-9, 1963.

Zeebe, R. and Wolf-Gladrow, D.: CO_2 in Seawater: Equilibrium, Kinetics, Isotopes, in: Oceanography Book Series, vol. 65, Amsterdam, 346, 2001.

675   Zhang, H., Stoll, H., Bolton, C., Jin, X., and Liu, C.: Technical note: A refinement of coccolith separation methods: Measuring the sinking characteristics of coccoliths, Biogeosciences, 15, 4759–4775, https://doi.org/10.5194/bg-15-4759-2018, 2018.

Zhang, H., Liu, C., Mejía, L. M., and Stoll, H.: Technical note: Accelerate coccolith size separation via repeated centrifugation, Biogeosciences, 18, 1909–1916, https://doi.org/10.5194/bg-18-1909-2021, 2021.

680   Zhang, Y. G., Pearson, A., Benthien, A., Dong, L., Huybers, P., Liu, X., and Pagani, M.: Refining the alkenone-pCO2 method I: Lessons from the Quaternary glacial cycles, Geochim Cosmochim Acta, 260, 177–191, https://doi.org/10.1016/j.gca.2019.06.032, 2019.

Zhang, Y. G., Henderiks, J., and Liu, X.: Refining the alkenone-pCO2 method II: Towards resolving the physiological parameter 'b,' Geochim Cosmochim Acta, 281, 118–134, https://doi.org/10.1016/j.gca.2020.05.002, 2020.

685 Ziveri, P., Stoll, H., Probert, I., Klaas, C., Geisen, M., Ganssen, G., and Young, J.: Stable isotope "vital effects" in coccolith calcite, Earth Planet Sci Lett, 210, 137–149, https://doi.org/10.1016/S0012-821X(03)00101-8, 2003.